Characterization of Constrained Swelling of Clay

JACOB UZAN, RAPHAEL BAKER, AND SAM FRYDMAN

Described in the paper are the development and application of a simple approach for estimating the response of a swelling soil profile to the percolation of surface water. The approach is made up of two parts: (a) A model for the flow regime, to predict the development of the wetted zone with time. It is used to predict the lateral extent and the vertical penetration of the wetting front for a surface wetting source of finite extent. (b) A model for the swelling process under constrained conditions. It is used to predict the surface heave of a swelling clay profile as a function of the extent of the wetted zone, and induced lateral and vertical constraints. The approach is illustrated by reference to the prediction of the development of heave with time in a swelling marl profile. The swelling parameters of the marl were obtained from laboratory tests in which radial as well as vertical stresses were measured. It is shown that the effect of confinement and limited extent of surface wetting source, often neglected in standard one-dimensional analysis, may be of major significance in limiting the heave that will develop in the field.

Evaluation of the response of swelling clay soils to the combined effects of wetting and mechanical constraints constitutes a formidable geotechnical problem. A complete solution of such a problem requires the study of saturated-unsaturated flow and its coupling with the swelling and stress-strain response of the material. The present state of knowledge does not allow such a comprehensive treatment but there exists, nevertheless, the need to estimate (even approximately) the expected response of a constrained clay layer to wetting.

The present paper describes the development of a model allowing the estimation of the combined effects of wetting from a surface source and mechanical constraint. The model is based on the following simplifying assumptions:

1. Decoupling of the flow and stress-strain problems. As a result of this decoupling, phenomena such as the effect of volume change on permeability, stress changes on suction, or suction changes on deformation moduli are not explicitly considered.
2. Representation of the continuous transition between the saturated and unsaturated flow regimes by a sharp wetting front advancing in time and space. As a result of this approximation, a volume element can exist only in one of two states: the initial (unwetted) state with degree of saturation S_o or a final saturated state with complete saturation, that is, $S_f = 1$.
3. Volume changes on wetting at constant stress and volume change due to stress change without wetting are assumed to be additive. Such an assumption is essentially a statement of a superposition principle between the free swell and stress-strain problems. This assumption results in a model that is similar to the one used in thermoelasticity, with volume changes due to wetting playing the role of thermal expansion.

On the basis of these assumptions, models for the flow regime and constrained wetting process are developed and used to illustrate the effect of extent of the wetted zone and of lateral constraint on the heave of a swelling marl profile covered by a nonswelling rock layer. The complete case study of feasibility of siting a nuclear power plant on such a profile is presented in a separate paper *(1)*.

A MODEL FOR THE FLOW REGIME

A comprehensive solution for the development of the wetted zone with time requires the solution of a complicated nonlinear partial differential equation describing saturated-unsaturated flow. Finite element programs for this purpose are available [e.g., Neuman *(2)* and Neuman et al. *(3)*], but these require parameter evaluation using nonroutine testing, and significant amounts of computer time. For the present simplified scheme, an approximate approach is used to obtain a solution for the development of the wetted zone. The solution contains two elements, one concerning the lateral extent of the wetted zone as a function of depth, and the other describing the vertical penetration of the wetting front with time. These two elements are discussed in the following paragraphs.

The Lateral Extent of the Wetted Zone

Use is made of an analytical solution for steady state flow of water from a ditch to a deep water table through homogeneous material, as presented by Harr *(4)* based on a derivation by Vedernikov *(5)*. Although this solution is for a two-dimensional case, it is also taken as a first approximation for axisymmetric conditions. A more complete discussion of Vedernikov's solution was presented by Baker et al. *(6)*. This solution may be expressed in the following form:

$$\frac{r - r_o}{H} = \left\{ \left(P_r\right)^{1/2} \left[1 - \exp\left(-\frac{\pi z}{2H}\right)\right]\right\} \quad (1)$$

where

r = lateral extent of wetted zone at depth z;
r_o = lateral extent of wetting source at surface;

Faculty of Civil Engineering, Technion-Israel Institute of Technology, Technion City, Mt. Carmel, Haifa 32000, Israel.

P_r = Permeability ratio; that is, ratio between horizontal and vertical coefficients of permeability; and
H = height of ponded water.

From Equation 1 it is seen that $(r - r_o)$ approaches a vertical asymptote at a radial distance equal to $H(P_r)^{1/2}$.

Vertical Penetration of the Wetting Front

The rate of penetration of the wetting front has been analyzed on the basis of one-dimensional vertical flow. In order to avoid the need for the solution of the nonlinear infiltration equation, the present approach is based on the assumption that the wetting process involves the advance of a sharp wetting front, that is, the material above the wetting front is assumed fully saturated and below the wetting front the degree of saturation equals its initial value. A similar assumption has been made by Bear *(7)*. Validity of this approximation was discussed by Baker et al. *(6)*.

Schematic profiles of degrees of saturation, S, and suction, ψ, as a function of depth, z, at a given time t, are shown in Figure 1. The full lines represent the complete infiltration solution, while the dashed lines correspond to the wetting front approximation used in the present analysis. As can be seen, the suction at the wetting front is not well defined, and a value of $\psi = \psi_o/2$ is used as a reasonable approximation. The profile is assumed homogeneous, with a constant value of ψ_o below the wetting front.

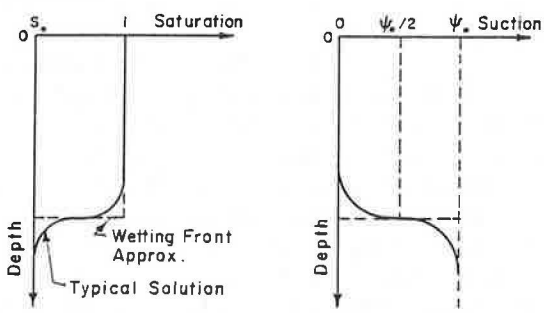

FIGURE 1 Degree of saturation and suction versus depth.

Following the analysis presented by Baker *(8)*, the following relation can be derived:

$$T = y - \ln(1 - y) \tag{2}$$

where y and T are nondimensional depth and time, respectively, defined as follows:

$$y = z/\overline{H} \tag{3a}$$

$$T = kt/n(1 - S_o)\overline{H} \tag{3b}$$

where

z = depth to the wetting front,
$\overline{H}$ = $h_c + \psi_o/2\gamma_w$,
h_c = thickness of the cracked zone,
ψ_o = initial suction in the unsaturated zone,
γ_w = unit weight of water,
k = the saturated coefficient of permeability,
t = time,
n = porosity, and
S_o = initial degree of saturation below the wetting front.

This solution applies to a homogeneous profile. An extension of the above approach to the case of a two-layered system has been developed using the concept of an equivalent coefficient of permeability. The solution is given by the expression

$$T = y - (B + 1)\ln(1 + y) + A \tag{4}$$

where

$$B = \overline{d}/\overline{H}\,(1 - k_2/k_1) \tag{5a}$$

$$A = \left[\left(\frac{n_1}{n_2}\right)\left(\frac{1 - S_1}{1 - S_2}\right)\left(\frac{k_2}{k_1}\right) - 1\right] \cdot \left[\frac{\overline{d}}{\overline{H}} - \ln\left(1 + \frac{\overline{d}}{\overline{H}}\right)\right] + B\ln\left(1 + \frac{\overline{d}}{\overline{H}}\right) \tag{5b}$$

where

$\overline{d}$ = thickness of upper layer,
k_1, n_1, S_1 = parameters of the upper layer, and
k_2, n_2, S_2 = parameters of the lower layer.

Equation 4 is valid for the case where the lower layer is less permeable than the upper one; otherwise there is no guarantee that the material in the bottom layer will be saturated.

Figure 2 shows the depth of the wetting front as a function of time for a particular choice of parameters. The shape of the wetted zone at different times is shown in Figure 3.

A MODEL FOR THE SWELLING PROCESS

The volume change of a soil element is a function of changes in the effective stress tensor acting on the element. This dependence may be expressed as a relationship between the void ratio e of the element, and the two components of the effective stress tensor: the mean effective normal stress, σ_m', and the deviational shear stress, τ_m [e.g., Newmark *(9)*]:

$$e = f_o(\sigma_m', \tau_m) \tag{6}$$

At levels of shear stress that are low relative to failure conditions, the void ratio change may be considered a function mainly of σ_m' [Henkel *(10)*, Frydman et al. *(11)*], and Equation 6 may be written approximately

$$e = f_1(\sigma_m') \tag{7}$$

It may be noted that Equation 7 describes the behavior of isotropic elastic materials in which volume change is dependent on changes in mean normal stress only. The effective normal stress, σ', in an unsaturated soil under drained conditions may be expressed in terms of the total stress, σ, and the water suction, ψ, as follows [see, for example, Bishop et al. *(12)*]:

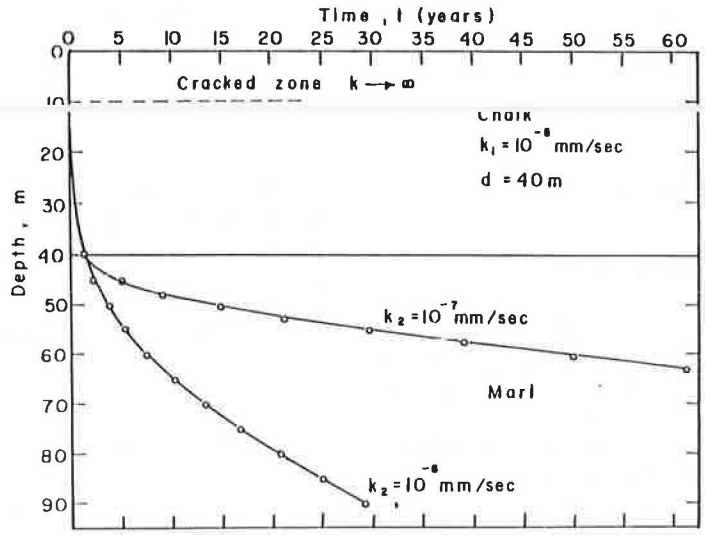

FIGURE 2 Position of wetting front as a function of time.

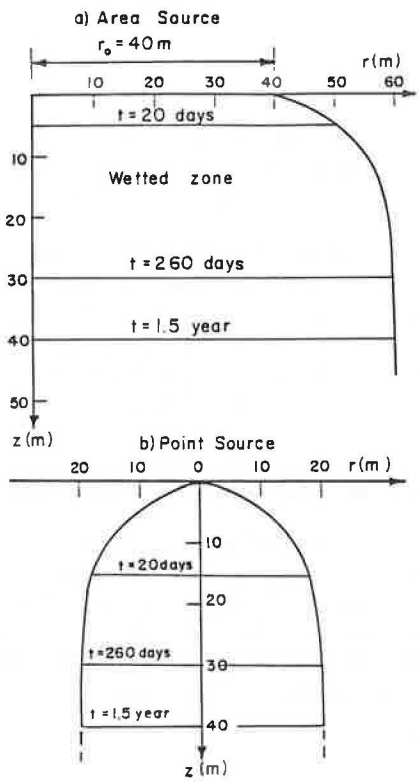

FIGURE 3 Shape of wetted zone at different times.

$$\sigma' = \sigma + \chi\psi \tag{8}$$

where χ is a soil parameter, dependent mainly on the degree of saturation of the soil, S. The suction, ψ, may also be assumed to be a function of the degree of saturation, S [Bear *(7)*]. Consequently, Equations 7 and 8 may be rewritten as

$$\sigma' = f_2(\sigma, S) \tag{9a}$$

$$e = f_3(\sigma_m, S) \tag{9b}$$

Therefore, the change in void ratio, de, may be expressed by

$$de = \frac{\partial e}{\partial \sigma_m} d\sigma_m + \frac{\partial e}{\partial S} dS = de_s + de_\sigma \tag{10}$$

that is, during a process that may involve wetting and change in applied stress, the total change in void ratio is the sum of two components—one due to the change in applied mean stress at constant degree of saturation (de_s), and the other due to change in the degree of saturation at constant mean stress (de_σ).

A similar approach has been presented by Picornell and Lytton *(13)*, except that they expressed de as a function of σ_m and ψ instead of σ_m and S; the approaches are equivalent. Justo et al. *(14)* also used a similar approach, but they applied to one-dimensional model and related void ratio changes to changes in vertical stress, σ_z, rather than mean normal stress, σ_m. It is, however, well accepted now that a three-dimensional approach is more representative of field conditions.

The wetting front approximation used for the analysis of the flow regime implies that a material element can exist only in one of two distinct saturation states. In the unwetted zone, $S = S_o$, the initial degree of saturation, and in the wetted zone, $S = 1$, and the material is fully saturated.

Figure 4 shows two curves representing the relationship between e and $\log \sigma_m$ for a clay soil element being compressed; curve *ABC* is for the soil at its natural moisture content, while curve *DEF* is for the saturated condition (i.e., $S = 100$ percent). The straight-line relationship for the saturated soil may be expressed as follows:

$$de_s = e_f - e_i = -\lambda \log [(\sigma_m)_f/(\sigma_m)_i] \tag{11}$$

where λ is a compression index, analogous to C_c or C_e, which relates e to σ_z in a one-dimensional process, and the subscripts f and i refer to final and initial conditions, respectively.

Point *B* represents the initial conditions of an unsaturated soil element that has a degree of saturation S_o and a void ratio e_o. If this element is wetted and allowed to swell under constant mean normal stress, a vertical path will be followed from point *B*; if the element becomes 100 percent saturated, it is assumed that it will reach point *D* and the change in void ratio is shown

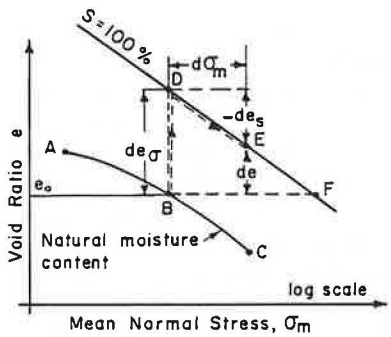

FIGURE 4 Void ratio: mean normal stress curves for wetted and unwetted marl.

on the figure as de_σ. If, on the other hand, the element is wetted under completely constrained conditions so that the volume cannot change, the state of the element will follow a horizontal path from point *B*; if full saturation is achieved, it is assumed that the element will reach point *F*, which defines the swelling pressure of the soil. Under field conditions, an element of soil will generally swell under partially confined conditions; in this case increase in void ratio will be accompanied by an increase in σ_m. If the element becomes fully saturated, it will reach the $S = 100$ percent curve at some point *E* between *D* and *F*. The void ratio change during such a process will be *de* and the stress increase $d\sigma_m$ as shown on the figure; this value is seen to be the sum of de_σ resulting from swell under constant σ_m and de_s resulting from compression at constant *S*, as expressed by Equation 10.

The analogy between the model already described for swelling of soils and that for a thermoelastic material is apparent. The void ratio change de_σ (path *BD*), which results from a change in the degree of saturation at constant stress, corresponds to volume change due to a change in temperature, *dT*. The void ratio change de_s (path *DE*), which results from a change in the state of stress at a constant degree of saturation ($S = 100$ percent), can be evaluated using conventional elastic stress analysis. Any arbitrary path *BE*, which is followed during a partially restrained process, may be considered as a superposition of paths *BD* and *DE*.

The model described previously is in the spirit of Jennings' *(15)* "double-oedometer" approach, with proper three-dimensional generalization. The formal correspondence between the swelling and thermal models is based on the expressions for volumetric strains in both models:

Swelling model $$\varepsilon_v = -\frac{1}{1+e_o}\, de_\sigma \tag{12a}$$

Thermal model $$\varepsilon_v = -3\alpha\, dT \tag{12b}$$

where α equals coefficient of linear thermal expansion, and ε_v equals volumetric strain (compression positive).

On the basis of Equations 12a and 12b, the following relation holds

$$\frac{de_\sigma}{1+e_o} = 3\alpha\, dT \tag{12c}$$

It is important to note that only the product *dT*, rather than the individual parameters α and *dT*, have a physical significance in terms of the present analogy; that is, any choice of α and *dT* which satisfies Equation 12c is equally valid. For convenience the following choice of parameters is made:

$$dT = de_\sigma \tag{13a}$$

$$\alpha = \frac{1}{3(1+e_o)} \tag{13b}$$

Equations 13a and 13b formalize the swelling-thermal analogy.

The second part of the model is based on the path *DE*; for this path, from Equation 11:

$$\varepsilon_v = -\frac{de_s}{1+e_o} = \frac{\lambda}{1+e_o}\log\left[1+\frac{d\sigma_m}{(\sigma_m)_i}\right] \tag{14}$$

Assuming an elastic model for compression at constant *S*, we have:

$$\varepsilon_v = \frac{d\sigma_m}{K} = \frac{3(1-2\mu)}{E}\, d\sigma_m \tag{15}$$

where *K* is the bulk modulus and *E* and μ are the modulus of elasticity and Poisson's ratio, respectively, of the saturated soil.

Combining Equations 14 and 15:

$$E = E(\sigma_m) = \left[\frac{3(1-2\mu)}{\lambda}\right](1+e_o)\left\{\frac{d\sigma_m}{\log[1+d\sigma_m/(\sigma_m)_i]}\right\} \tag{16}$$

If the Poisson's ratio is assumed to be constant, then the present model for the swelling of soils implies a nonlinear thermoelastic material with the modulus of elasticity, *E*, dependent on the mean normal stress (σ_m).

The complete swelling-elastic model is governed by the following system of equations for the axisymmetric case:

$$\varepsilon_z = \frac{1}{E}(d\sigma_z - 2\mu d\sigma_r) - \alpha de_\sigma \tag{17a}$$

$$\varepsilon_r = \varepsilon_\theta = \frac{1}{E}[d\sigma_r - \mu(d\sigma_r + d\sigma_z)] - \alpha de_\sigma \tag{17b}$$

The parameters μ, α, λ, and the function $de_\sigma = de_\sigma(\sigma_m)$ are evaluated on the basis of laboratory tests, as described in the following section.

EVALUATION OF GEOTECHNICAL PARAMETERS

In order to apply the procedure described previously, it is necessary to establish values for the following geotechnical parameters:

1. Flow Parameters: The coefficient of permeability *k*, porosity *n*, degree of saturation S_o, and in situ suction ψ_o in both the overlying layer and the swelling layer. A simplified analysis may be based on a constant ψ_o.
2. Heave Parameters: The elastic parameters *E* and μ for the overlying nonswelling material, and for the unwetted swelling soil. For the wetted swelling soil λ, μ, and e_o are needed for evaluation of the coefficient of linear expansion α (Equation

13b) and E = E (σ_m) (Equation 16). In addition, it is necessary to establish the function $dT = de_\sigma = de\ (\sigma_m)$ for the wetted swelling material.

The following presents an illustration of application of the model to the case of a swelling marl profile overlain by a 40-m-thick chalk layer.

Flow Parameters: Coefficients of permeability of the saturated marl were obtained from laboratory consolidation tests. These values were found to be in the range 10^{-7} to 10^{-9} mm/sec. In view of the possibility that fine crack patterns and foreign lenses within the marl would result in higher permeabilities for the en masse material, it was decided to carry out the analyses using values of $k = 10^{-7}$ mm/sec and 10^{-6} mm/sec; these values, on the high side, are conservative, as they will result in more rapid wetting and swell of the marl and consequent heave of the profile surface.

Values of n measured on core samples of the marl lay between 25 percent and 42 percent, and a value of n = 37.5 percent was adopted for the present analyses. The degree of saturation, S_o, of these cores varied between 75 percent and 95 percent, and a value of S_o = 85 percent was adopted.

Figure 5 shows laboratory suction curves obtained for two marl cores taken from within 3 m of the top of the marl layer. The in situ moisture content in this region was of the order of 20 percent; consequently, the value of ψ_o in the laboratory condition (without overburden pressure) was of the order of 2.0–2.5 MPa. The corresponding in situ value was obtained by subtracting the effect of overburden pressure [Croney et al. *(16)*], yielding a range of ψ_o = 0.4–1.5 MPa through the marl profile. A representative value of ψ_o = 1.0 MPa was chosen for the analysis.

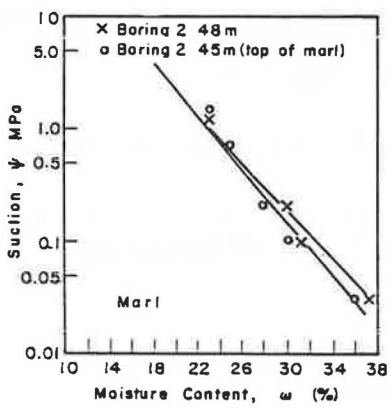

FIGURE 5 Suction curves from pressure plate tests for marl.

Elastic parameters of unwetted marl: Values of E and μ were obtained from the initial stages of one-dimensional confined compression tests in which samples were later wetted in order to study swelling. The tests were performed in special consolidometer rings instrumented with circumferential strain gauges [Komornik and Zeitlen *(17)*], enabling measurement of change in radial stress ($\Delta\sigma_r$) accompanying changes in vertical stress ($\Delta\sigma_z$) and swelling. Assuming linear elasticity, Equations 17, with $\alpha = 0$ and $\varepsilon_r = \varepsilon_o = 0$ may be used to evaluate parameters E and μ from results of these tests.

Tests were performed on specimens with dry densities varying from 15.2 kN/m^3 to 17.5 kN/m^3, and a wide range of E and μ values were obtained. Values of E = 300 kPa and μ = 0.35 (corresponding to a coefficient of earth pressure at rest, K_o of about 0.5) were chosen for the analysis.

Parameters of wetted marl: The elastic parameters E and μ and the swelling parameters and de_σ were obtained from one-dimensional confined swell and subsequent compression tests in which both vertical and radial stresses were measured. Figure 6 shows curves of e versus σ_m for four different marl samples in both the unwetted and the wetted states. Each curve is an average curve drawn through points obtained from tests on a number of specimens wetted after compression to different mean stresses; the wetted curves are drawn through points reached after swelling from the unwetted condition or after compression of previously wetted specimens.

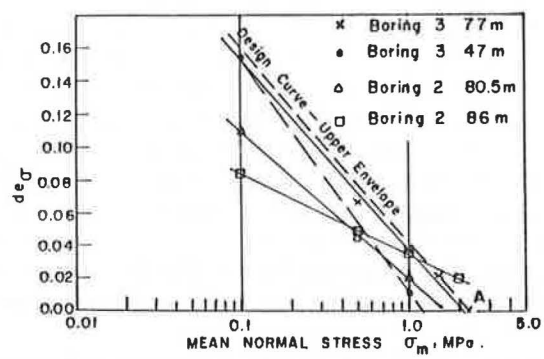

FIGURE 6 Laboratory $e - \sigma_m$ curves for marl samples.

For each set of curves, the vertical distance between the two curves represents de_σ for any particular σ_m. Figure 7 shows the relation $de_\sigma\ (\sigma_m)$ for the four samples. The upper envelope shown on the figure represents a conservative design curve.

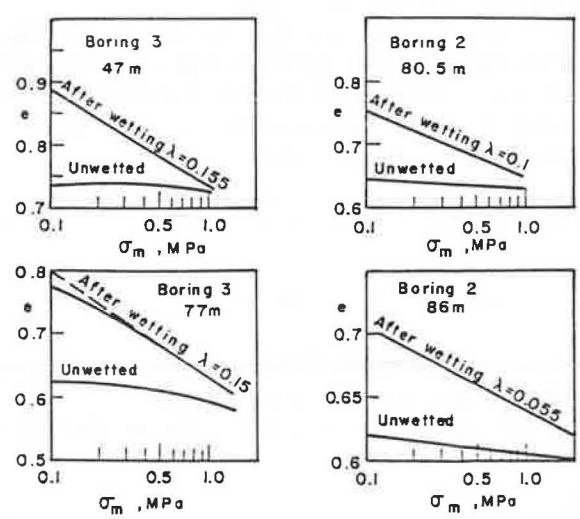

FIGURE 7 de_σ versus σ_m marl samples.

The sampling and testing program has indicated that values of e_o for the marl are consistently above 0.6 (see, for example, Figure 6). Because the swelling parameter α will be higher the lower the value of e_o, representing a more highly swelling material, a value of $e_o = 0.6$ is conservatively adopted for the present analyses, leading to $\alpha = 0.208$.

Results of swelling tests yielded values of μ between 0.1 and 0.3, and a value of 0.2 is adopted. E is assumed to be dependent on σ_m according to Equation 16, and is obtained from the wetted $e - \log \sigma_m$ curves in Figure 6. From these curves, λ was found to vary between 0.055 and 0.155. Adopting a value of $\lambda = 0.13$, and using the values of μ and e_o previously defined, E may be expressed as a function of $(\sigma_m)_i$ and $d\sigma_m$ through Equation 16. The depth corresponding to any value of $(\sigma_m)_i$ has been obtained by assuming an average profile total density γ of 18 kN/m^3 and a coefficient of earth pressure at rest, $K_o = 0.5$ in the unwetted marl.

NUMERICAL PROCEDURE

The models developed were used to study the effect of lateral restraint on heave. The profile analyzed consists of marl covered by a 40-m-thick chalk layer. The chalk layer is composed of an upper 10-m cracked (pervious) chalk and 30 m of sound chalk, with assumed coefficients of permeability 10^{-1} mm/sec and 10^{-5} mm/sec, respectively. A 40-mm diameter surface wetting source and a point source are considered.

Heave calculations are made using the finite element program SAP7 made available by the Israel Electric Co. Ltd. and developed by the Structural Mechanics Computer Laboratory, University of Southern California. Figure 8 shows a typical mesh. One run of the program involves calculation of the stress increments at the centers of the elements and the displacements at the nodes that result from wetting a particular depth of marl. For example, advance of the wetting front 10 m into the marl corresponds to wetting elements 41–46; this is input by specifying relevant values of de at nodes 45 to 51 and 56 to 62. If 20 m of marl are to be wet, values of de_σ are also specified at nodes 67 to 73, and so on. The input values of de_σ are a function of the initial mean stress, $(\sigma_m)_i$ at the node according to Figure 7, $(\sigma_m)_i$ being given by

$$(\sigma_m)_i = \frac{\sigma_z + 2\sigma_r}{3} = \frac{1 + 2K_o}{3}\gamma z \tag{18}$$

As the thermoelastic model employed here is nonlinear (the modulus of elasticity E depends on σ_m), it is necessary to use the finite element procedure iteratively. This was done in the following manner: as a result of a run, a value of $d\sigma_m$ is obtained at the center of each wetted marl element, a new E value is calculated and a new run carried out. The process is repeated until the change in E of all wetted marl elements is no greater than 5 percent; this usually requires two or three iterations.

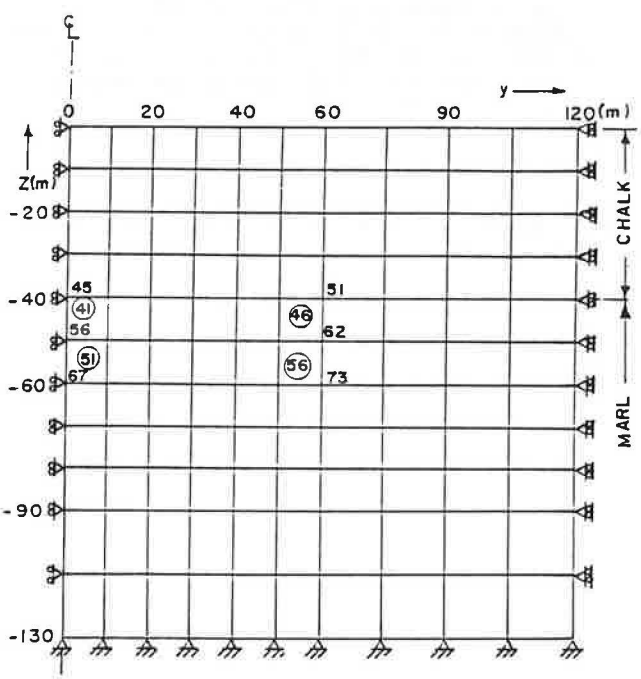

FIGURE 8 Typical finite element mesh—40-m chalk.

RESULTS

A preliminary estimate of the expected surface heave, based on one-dimensional analysis (i.e., wetting extends to infinity in the horizontal direction and the constraining effect of the chalk because of its flexural rigidity is not considered), gave results of the order of 750 mm. This value represents an upper limit to the heave.

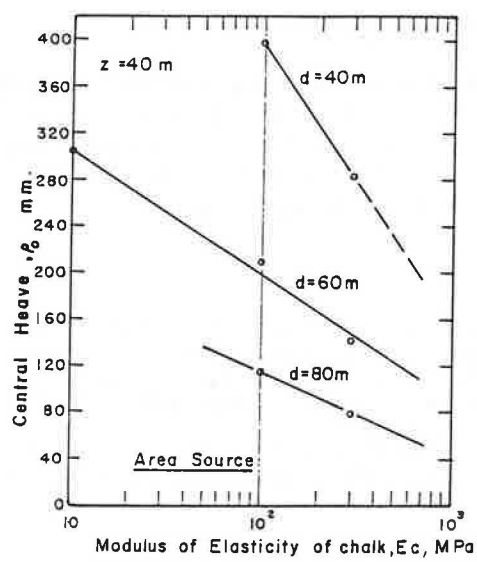

FIGURE 9 Influence of E_c on central heave.

Figure 9 shows the effect of chalk modulus of elasticity, E_c, on the central heave for a penetration of the wetting front 40 m into marl. The time for the wetting front to penetrate 40 m into the marl, resulting in the heave shown in Figure 9, may be obtained by reference to Figure 2. It is seen that for an assumed coefficient of permeability of marl $k_m = 10^{-7}$ mm/sec, infinite time is needed, while for $k_m = 10^{-6}$, the heave would develop after 20 years. In a similar way, values of central surface heaves may be obtained at various times (i.e., for different depths of

infiltration into the marl) following the start of wetting, for any values of chalk modulus of elasticity and chalk thickness; results of such a study are presented in an accompanying paper (7). Considering that a representative value of the en masse modulus of elasticity of chalk would be expected to be of the order of 500 MPa (7), Figure 9 indicates that for $k_m = 10^{-7}$ mm/sec, a maximum heave of about 230 mm would be expected for a 40-m diameter surface wetting source—that is, about one-third of that estimated on the basis of one-dimensional swell analysis. In the case of a point wetting source, a central surface heave of only 23 mm would be predicted. This illustrates the extent of overestimation that may result from the one-dimensional analysis.

CONCLUSIONS

An approach has been developed and presented for the estimation of the surface heave to be expected at a swelling soil site. The approach is conservative in the it assumes the availability of an unlimited supply of water at the surface and the development of full saturation within the wetted zone.

The approach presented has been applied in the paper to the analysis of a particular profile, but it may be used to provide a conservative estimate of heave at any swelling soil site. It is shown that the effect of confinement and limited extent of surface wetting source, often neglected in standard one-dimensional analyses, may be of major significance in limiting the heave that will develop in the field.

ACKNOWLEDGMENT

The work described in this paper was carried out for the Israel Electric Co. Ltd., whose permission to publish the paper is gratefully acknowledged. The cooperation and encouragement of A. Kidron, I. Kiss, and S. Denekamp of the Israel Electric Co. Ltd. are particularly appreciated.

REFERENCES

1. S. Frydman, R. Baker, and J. Uzan. Constrained Swelling of Clay—A Case Study (in preparation).
2. S. P. Neuman. Saturated-Unsaturated Seepage by Finite Elements. *Journal of the Hydraulic Division*, ASCE, Vol. 99, No. HY12, 1973, pp. 2233–2250.
3. S. P. Neuman, R. A. Feddes, and E. Bresler. *Finite Element Simulation of Flow in Saturated-Unsaturated Soils Considering Water Uptake by Plants*. Third Annual Report, Project ALO-SWC-77. Technion-Israel Institute of Technology, Hydraulic Engineering Laboratory, 1974.
4. M. E. Harr. *Groundwater and Seepage*. McGraw Hill, New York, 1962.
5. V. V. Vedernikov. Seepage from Channels. *Wasserkraft and Wasserwirtschaft*, No. 11, 1934.
6. R. Baker, S. Frydman, and G. Wiseman. *Geotechnical Considerations in the Design and Construction of Earth Reservoirs*. Research Report, Technion-Israel Institute of Technology, Area of Geotechnical Engineering, 1984 (in Hebrew).
7. J. Bear. *Dynamics of Fluids in Porous Media*. Elsevier Science Publishers, Amsterdam, The Netherlands, 1972.
8. R. Baker. Seepage Losses from Small Irrigation Reservoirs. *Proc., 11th International Conference on Soil Mechanics Foundation Engineering*, San Francisco, Vol. III, 1985, pp. 1179–1182.
9. N. M. Newmark. Failure Hypotheses for Soils. *Proc., ASCE Research Conference on Shear Strength of Cohesive Soils*, Boulder, Colo., 1960, pp. 17–32.
10. D. J. Henkel. The Relationships Between the Effective Stresses and Water Content in Saturated Clay. *Geotechnique*, Vol. 1, 1960, pp. 41–54.
11. S. Frydman, J. G. Zeitlen, and I. Alpan. The Yielding Behaviour of Particulate Media. *Canadian Geotechnical Journal*, Vol. 10, No. 3, 1973, pp. 341–362.
12. A. W. Bishop, I. Alpan, E. E. Blight, and I. B. Donald. Factors Controlling the Strength of Partly Saturated Cohesive Soils. *Proc., ASCE Research Conference on Shear Strength of Cohesive Soils*, Boulder, Colo., 1960, pp. 503–532.
13. M. Picornell and R. L. Lytton. Modelling the Heave of a Heavily Loaded Foundation. *Proc., Fifth International Conference on Expansive Soils*, Adelaide, Australia, 1984, pp. 104–108.
14. J. L. Justo, J. Saura, J. E. Rodriguez, A. Delgado, and A. Jamarillo. A Finite Element Method to Design and Calculate Pier Foundations in Expansive-Collapsing Soils. *Proc., Fifth International Conference on Expansive Soils*, Adelaide, Australia, 1984, pp. 119–123.
15. J. E. Jennings. The Theory and Practice of Construction on Partly Saturated Soils as Applied to South African Conditions. *Proc., First International Conference on Expansive Soils*, 1965, pp. 345–363.
16. D. Croney, J. D. Coleman, and W. P. M. Black. Movement and Distribution of Water in Soil in Relation to Highway Design and Performance. In *HRB Special Report 40*, HRB, National Research Council, Washington, D.C., 1958, pp. 226–252.
17. A. Komornik and J. G. Zeitlen. An Apparatus for Measuring Lateral Soil Swelling Pressure in the Laboratory. *Proc., 6th International Conference on Soil Mechanics Foundation Engineering*, Vol. 1, 1965, pp. 278–281.

Publication of this paper sponsored by Committee on Environmental Factors Except Frost.